# Assessment tools for numerical resolution of a contact dynamic problem with modal basis reduction.

T. Catterou, V. Blanc, G. Ricciardi, Stéphane Bourgeois, B. Cochelin

Available online at www.sciencedirect.com

ScienceDirect

Procedia Engineering 199 (2017) 540–545

Procedia Engineering

www.elsevier.com/locate/procedia

X International Conference on Structural Dynamics, EURODYN 2017

# Assessment tools for numerical resolution of a contact dynamic problem with modal basis reduction.

T.Catterou[1,3], V.Blanc[1], G. Ricciardi[2], S.Bourgeois[3], B.Cochelin[3]

[1] *CEA Cadarache – DEN/DEC/SESC/LC2I, 13108 Saint Paul lès Durance, France*
[2] *CEA Cadarache – DEN/DTN/STCP/LHC, 13108 Saint Paul lès Durance, France*
[3] *Aix Marseille Univ, CNRS, Centrale Marseille, LMA, Marseille, France*

**Abstract**

This paper is devoted to the study of the modal basis reduction method in the framework of the dynamical behavior of a mechanical system with multiple joint clearances. The final objective is to estimate contact forces in a confined tube bundle during a dynamic loading for nuclear components sizing. The modal basis reduction combined with an explicit integration scheme is envisioned to deal with the large number of tubes and potential contact zones. In this paper, method is first applied to the example of a clamped-free beam impacting on a spring on its free edge. A semi-analytical resolution allows assessing the validity of the modal basis reduction method depending of some parameters, like frequency truncation and ratio between the bending stiffness and the spring stiffness. This study leads to criteria on numerical parameters which have to be respected to ensure stability and accuracy of results.


Peer-review under responsibility of the organizing committee of EURODYN 2017.

*Keywords:* Dynamic; modal analysis; contact; finite-element.

**Nomenclature**

| | |
|---|---|
| $\boldsymbol{u}(x,t)$: Beam's bending | $\boldsymbol{M}, \boldsymbol{C}, \boldsymbol{K}$ **:** Mass, damping and stiffness matrices – physical basis |
| $u_0, v_0$: Initial displacement and velocity | $\boldsymbol{\Phi}$: Eigenvector matrix |
| $\boldsymbol{q_i}(t)$: Modal contribution - mode i | $\boldsymbol{\Phi_i}(\boldsymbol{x})$: Mode shape – mode i |
| Γ: Power spectral density | $K_s, K_b$ : Shock stiffness and damping, Bending stiffness |
| $SR_f$: Ratio of contact force integer | $R_k$ : Ratio of shock and bending stiffness. $(K_s/K_b)$ |
| $f_i$: frequency – mode i | $f_{trunc}$: Frequency truncation of numerical computation |
| $\xi_i$ : Structural damping – mode i | $R_{ftrunc}$: Ratio of $f_{trunc}$ and first natural mode frequency |

## 1. Introduction

### *1.1. Contacts in dynamical simulation*

Multibody collisions are one of the strongest non-linearity in mechanics. Contact modelling is an ancient topic, which started with works of Hertz in 1882 [1] on the contact between two optical lenses. Many authors have expanded thereafter this theory by introducing friction, tangential force and dynamic effects [2],[3]. But, the numeric implementation of contact condition remains

1877-7058 
Peer-review under responsibility of the organizing committee of EURODYN 2017.
10.1016/j.proeng.2017.09.154

very complex, whereas it is usually met in industrial context. Impacts occur during very brief time, and cause high forces and accelerations [4]. Standard numerical methods struggle to converge or to remain stable, leading to inaccurate or very slow calculations [5]. Several dedicated integration schemes have been created to solve contact problems, using a time-step cutting [6], energy consistency [7] or high frequency damping [8]. There are two main kinds of integration schemes, implicit ones which require an iterative process minimizing the error, and the explicit ones where the calculation is direct. In most cases, explicit schemes are more relevant to deal with contact issues, because they are faster than implicit ones and remain stable as long as time step is short [5]. But implicit schemes are sometimes used because of their accuracy for contact problem ([9], [10]).

The integration scheme choice and the manner to model contact are linked. Reference [4] summarizes main ways to model contact in structural dynamics; they are two major categories: non-smooth laws for which the contact is instantaneous and the velocity is discontinuous versus smooth laws for which the solids in contact will be able to interpenetrate each other. In non-smooth contact dynamics, a restitution parameter is introduced to model the damping ([11], [12], [13]) but does not allow to estimate contact forces. In smooth contact dynamics, a non-linear force is added to the other loads depending joint clearance between solids in contact [14]. Several formulations of the contact laws can be found in literature [4], from the expression of Hertz [1] until the most complicated formulation of Thornton [13]. These laws have been confronted to solve the Newton's cradle [15]. For now, a linear formulation is considered. Then, a modal basis reduction is used to decrease the size of the model [16] even if it's not commonly done for non-linear problem.

### *1.2. Industrial issue*

In sodium fast reactor (SFR), the fuel is enclosed in pins, composed of slender steel tubes (the sleeve) and a helical spacer wire around the sleeve. (Figure 1-a)

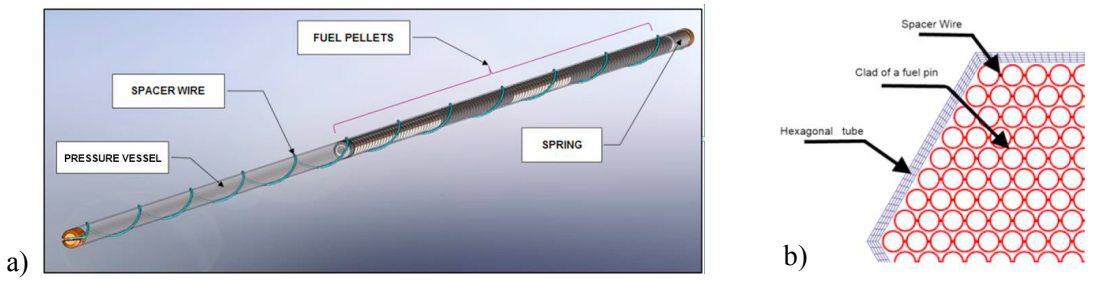


Figure 1 – ASTRID fuel pin (a) and cross section of the pins bundle in its hexagonal tube (b)

Fuel pins are arranged in a bundle enclosed inside a hexagonal tube (Figure 1-b). The whole forms fuel assemblies which are main constituents of the reactor core. During a dynamic load, assemblies impact each other locally on spacer pads. The shock generates acceleration on pins and cause dynamic stresses. At virgin state, clearances are nearly homogeneous in the bundle. During irradiation, clads swell due to thermal and pressure loads and clearances are also modified unevenly. The industrial aim is to develop a calculation methodology to identify contact forces caused by dynamic loads (earthquake, handling or transportation), throughout the life of assembly. Then, a local model will allow assessing maximum stresses in pins and sizing them. All calculations shown in the follow-up have been made with the finite-element software CAST3M [17] for numerical aspects and Scilab for reference computations.

This paper is the first step to simulate dynamic behavior of large structures made of large number of sub-structure in contact with clearance similar to our industrial case. First studies are made on a standard problem presented §**2**, for which semi-analytical results can be established (§**2.2**). Comparisons between analytical results and the modal basis reduction method result are made (§**2.4**) leads to identify the validity domains of the numerical methods with respect to key parameters.

## 2. Analysis of the numerical method on a simple contact problem

### *2.1. Presentation of the issue*

A simple contact problem is first considered: a cantilever beam initially bent at rest with null velocity and comes to impact on a spring at its free end (Figure 2) which has a stiffness $K_s$. The initial bent configuration is taken as the first vibration mode. . This case is similar to experiments realized at the CEA on the shock of an assembly filled with a tube bundle on a hard stop. Semi-analytical results are established and will be compared to numerical results obtained with the modal basis projection method.

All results will be observed according to the dimensionless factor $R_k$, ratio of spring and bending stiffnesses ($K_{shock}/K_{bend}$), with $K_{bend} = 3EI/L^3$. Numerical application are made for a beam with the following properties: $K_{bend} = 4{,}5.10^5 N/m$, total mass $m = 127kg$.

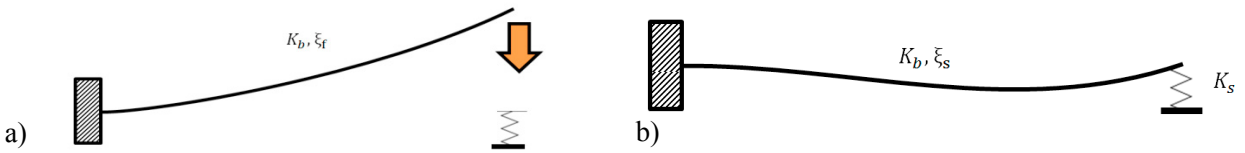


Figure 2 - Clamped beam impact on a spring. a) free edge - b) contact on the spring

*2.2. Semi-analytical reference solution*

The issue is split in two phases, when the end of the beam is free, and when the end is in contact with the spring. In each case, the linear problem is solved with modal reduction, by using the decomposition (1) on N modes whose natural frequencies are lower than frequency truncation $f_{trunc}$ :

$$\boldsymbol{u}(x,t) = \sum_{i=1}^{N} \Phi_i(x)\boldsymbol{q_i}(t), \tag{1}$$

The solution of the fundamental equation of dynamic on modal basis is given by (2):

$$q_i(t) = e^{-\xi_i \omega_i t}\,(A_i \cos(\omega_d t) + B_i \sin(\omega_d t)), \tag{2}$$

$$A_i = \frac{\int_\Omega u_0.\Phi_i}{\int_\Omega \Phi_i.\Phi_i}\;;\; B_i = \frac{\int_\Omega v_0.\Phi_i}{\omega_i \int_\Omega(\Phi_i.\Phi_i)} + \frac{\xi_i}{\omega_i\sqrt{1-\xi_i^2}}\,A_i \quad ; \quad \omega_d = \omega_i(1-\xi_i^2). \tag{3}$$

Eigen values $\omega_i$ can be found analytically. Computation is complex for the fixed-spring configuration, Refer to Behn [18] for a full resolution. The continuous expression (2) gives all the values of modal displacements for each configuration. The full displacement $u(x,t)$ can be calculated by using the expression (1). With this approach, the exact solution is unreachable, given that it requires decomposing the solution on infinity of modes, a truncation frequency $f_{trunc}$ is introduced on equation (1) which is choose arbitrarily high for comparison analysis in §2.4.

The main difficulty is to obtain transition times between the two configurations presented Figure 2. We will observe a configuration change when $u(L) = 0$, with $L$ the spring abscissa. A root finding algorithm, the secant method [19], is used to find the first time the displacement $u(L,t)$ becomes zero using formula (2). When the transition time is found accurately the configuration change, initial conditions $u_0$ and $v_0$ are updated (so are $A_i$ and $B_i$) and (2) gives the new equation to use in the following computation. Then the procedure is iterated until reaching a predetermined number of rebound or time. Finally, when all the contact and take off times are determined, the solution can be built using equations (2) for each phase. Attention must be given to damping parameters; they have to be calculated to ensure damping equivalence between both configurations.

The methodology allows us to simulate analytically the fall of a clamped beam on a spring. It's a novel approach which has the main advantage to solve a non-linear contact issue with continuous expressions using only beam theory hypothesis. This computation will be used as reference in §2.4 with the aim to assess the accuracy of numerical method (Figure 3).

*2.3. Modal basis reduction method*

The Equation of the Dynamics for a numerical issue is written (4), with $F_{shock}$ nonlinear contact forces.

$$\boldsymbol{M}\ddot{u}^t + \boldsymbol{C}\dot{u}^t + \boldsymbol{K}u^t = F^t + F^t_{shock}(u) \tag{4}$$

$$F_{shock} = k_c \Delta u(L)\ si\ \Delta u(L) < 0 \qquad F_{shock} = 0\ otherwise \tag{5}$$

Then, computation time is heavily linked to the size of the matrices $\boldsymbol{M}, \boldsymbol{K}\ and\ \boldsymbol{C}$ used. A way to reduce drastically the size of these matrices is to project them on the modal bases [20]. Modes are obtained by solving the equation (6):

$$(\boldsymbol{K} - \omega^2 \boldsymbol{M})\Phi = 0 \tag{6}$$

This calculation gives the eigenvalues $\omega$ and the eigenvectors $\Phi$ of the structure without contact. Unlike the analytical solution, only the clamped free modal basis is used, the spring effect is moved to the right hand-side of the equation (4). The displacement of the structure can be divided for each mode by using (1), with a certain frequency truncation which will be discussed in §2.4. The equation of the dynamic (4) can be re-written using the decomposition (1) :

$$\boldsymbol{\Phi^t M \Phi \ddot{q}} + \boldsymbol{\Phi^t C \Phi \dot{q}} + \boldsymbol{\Phi^t K \Phi q} = \boldsymbol{\Phi^t F_{ext}} + \boldsymbol{\Phi^t F_{shock}(u)} \tag{7}$$

By construction, matrices $\bar{\boldsymbol{M}} = \Phi^t \boldsymbol{M} \Phi$ and $\bar{\boldsymbol{K}} = \Phi^t \boldsymbol{K} \Phi$ are diagonal.

The contact force is defined on "physical" basis. So during the computation, physical displacement of each contact point is calculated, contact forces are deducted from these displacements and contact force are projected on the set of modal basis [21].

For the computation, a classical central difference integration scheme is used. It allows very fast calculations, but requires using an appropriate time step to ensure stability.

### *2.4. Assessment tools and comparison analytical/numerical computation*

Figure 3 shows the displacement of the right end of the beam during time obtained by numerical or analytical method. A dimensionless ratio is used in following studies: $R_{ftrunc} = f_{trunc}/f_1$, ratio between the frequency truncation and the frequency of the first natural mode. Numerical computation results concurs with reference ones when $R_{ftrunc}$ is high (Figure 3 – b). Some assessment tools are necessary to quantify differences between numerical results and references ones.

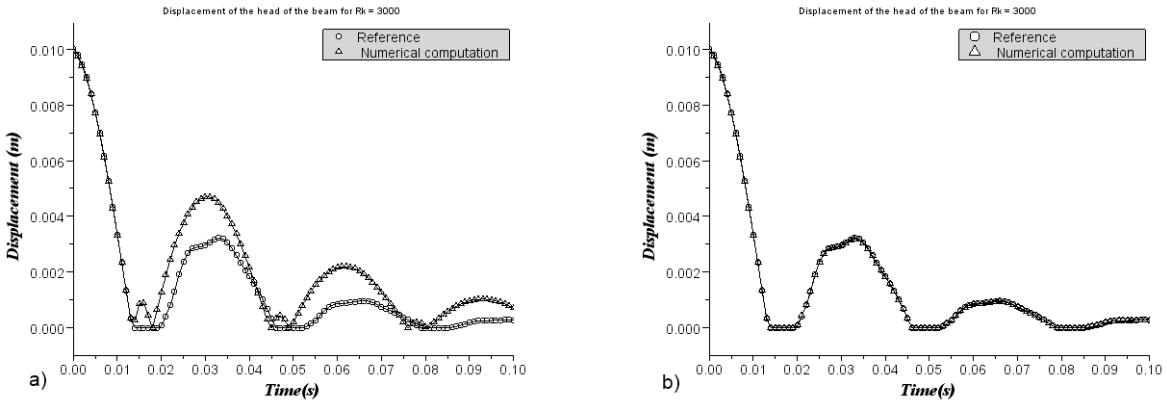


Figure 3 - Displacements on the beam's edge for numerical computation and analytical standard - a) $R_{ftrunc}$ = 10, $R_k$=3000, $Err$ =35%. b) $R_{ftrunc}$ = 300, $R_k$=3000, $Err$ =3%

An error function $Err(R_k)$ (8) is introduced. It quantifies differences between power spectral densities $\Gamma_{\text{num}}$ and $\Gamma_{ref}$ obtained with the two methods and it falls between 0% (superposed signals) and 100% (decorrelated signals)

$$\text{Err} = \frac{\max(|\Gamma_{num} - \Gamma_{ref}|)}{\max([|\Gamma_{num}|, |\Gamma_{ref}|])} \tag{8}$$

This function accounts for the correlation between numerical curves and reference ones and is plotted Figure 4 – a). It is globally responsive to amplitude or phase error, but doesn't take into account short signal variations induced by contact.Thus, another assessment tool based on the ratio of contact forces integrated on the first shock time is proposed Eq. (9) and is defined between 1 (same contact forces) and 0 (contact forces infinitely distinct), see Figure 4 – b.:

$$\text{SR}_\text{f} = \frac{\min\left(\int_{shock1} \boldsymbol{F}_{shock_{num}}, \int_{shock1} \boldsymbol{F}_{shock_{ref}}\right)}{\max\left(\int_{shock1} \boldsymbol{F}_{shock_{num}}, \int_{shock1} \boldsymbol{F}_{shock_{ref}}\right)}, \tag{9}$$

First, one must note that explicit schemes have a standard criterion to avoid divergence [5] : $dt < 1/4 f_{trunc}$. The function $Err$ and $\text{SR}_\text{f}$ are plotted Figure 4, depending of the stiffness ratio, for various modal truncation ratio. Same functions are plotted

for computations with a classical implicit scheme (average acceleration method) without modal reduction. Note that implicit problem solving is at least 30 times slower with equal spatial discretization.

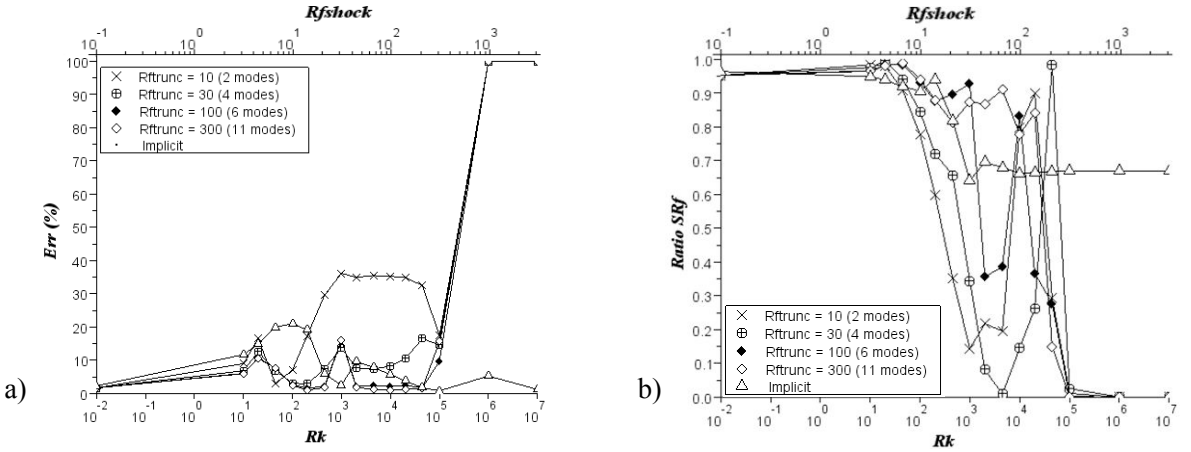


Figure 4 – a) Error function $Err$ and b) ratio $SR_f$ depending on modal truncation $R_{ftrunc}$ and $R_k$ ratio

For a low modal truncation ($R_{ftrunc} = 10$) and a ratio $R_k$ higher than $10^2$, the "error" $Err$ is about 35% (Figure 4 - a). It represents an overvaluation of the amplitude of about 30% and a phase offset (Figure 3-a). With a higher modal truncation ($R_{ftrunc} = 300$), analytical and numerical displacements are more or less the same and the error function is close to zero (Figure 3-b). In term of contact force, numerical model gives similarly very bad results for low frequency truncation, since $R_k > 10^2$. Moreover, Figure 4 – b) shows that when $R_k$ is high (>$10^3$), a ratio $R_{ftrunc} = 300$ is necessary to give an acceptable estimate of the contact force ($SR_f > 0{,}8$). Classical computations with implicit scheme give poor results for a hard contact due to the larger time discretization. When $R_k$ is very high (> $10^5$ here, but the value is dependant of the time step chosen), numerical computations diverges with explicit scheme, contrary to an implicit computation as observed in [22] (Figure 4-a).

With further examination, you can assess than computation is approximately accurate when the criterion (10) is respected:

$$Rf_{trunc} > \frac{f_{shock}}{f_1} = R_{fshock} = \sqrt{R_k}$$
$$f_{shock} = \frac{1}{t_{shock}} \approx \frac{1}{2\pi}\sqrt{\frac{K_{shock}}{m}},\ f_1 = \frac{1}{2\pi}\sqrt{\frac{3EI}{L^3}} \quad (10)$$

$f_{shock}$ corresponds to the frequency of the shock of a mass $m$ on a spring of stiffness $K_s$. Figure 4-a shows that error $Err$ starts to raise when $Rf_{shock} > Rf_{trunc}$.The standard criterion on explicit scheme, the shock frequency criterion (10) and the Figure 4 – b give us several recommendation for the choice of $f_{trunc}$ (11).

$$\frac{1}{4\ dt\ f_1} > R_{ftrunc} > \sqrt{R_k} \text{ and } R_{ftrunc} > 300\ if\ R_k > 10^2\ . \quad (11)$$

## 3. Extension to a 2D multicontact problem.

This methodology is now applied on the larger structure presented in §1.2. (Figure 5 – a)). It's an extension of the simple problem treated in §0, the beam impacting is a hexagonal tube containing a pin bundle with clearance. The hexagonal tube and each tube of the bundle are modelled as a beam. Due to pin's wire, locations of potential contact zones are known, and a unilateral condition (5) can be integrated for each zone. Computation is made with a set of modal basis, one basis for each pin. During the dynamical calculation, all contact force conditions are checked during each time step, and the force vector is updated for the following time step. Considering that contact forces are calculated for a large number of time step, it is easy to retain values of these forces and to use them for sizing purpose (Figure 5-b). This numerical methodology, as described in §2.3, allows very fast computation (around 30s for the calculation shown Figure 5) and lead to accurate results as soon as the choice of numerical parameters is appropriate. Knowing material and geometrical properties of the system, criteria given in this paper and in studies on time step and spatial discretization enable to choose best numerical parameters for computation.

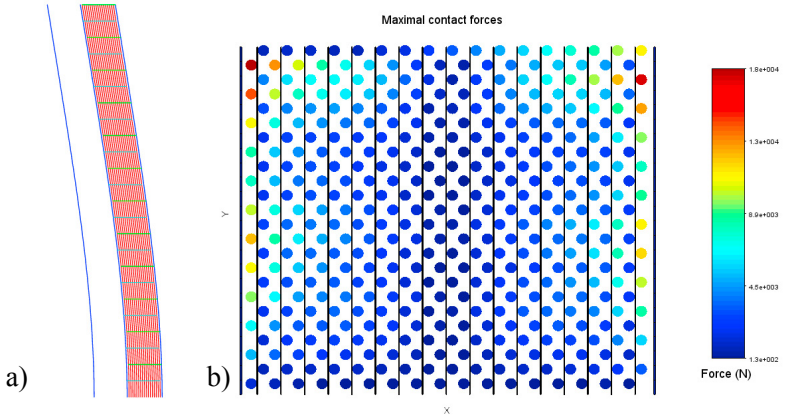


Figure 5 - a) 2D Finite element model of an assembly containing a tube bundle, b) Schematic representation of maximal contact force during a dynamic load.

## 4. Conclusion

In this paper, we investigated some criteria to assess the validity of the modal basis reduction method on a simple contact problem for which a semi-analytical resolution can be established. Influence of numerical modal truncation has been analyzed, and this leads to advice to choose the optimal value of this parameter. The same kind of studies can be made on the influence of time and spatial discretization. It leads us to build a validity domain of the modal basis reduction method, which will allow us to choose best numerical parameters to provide both a good accuracy and fast computation, even for complex problem. The next step will be to use these criteria on several structures with clearance as the problem presented in this paper.

## References

[1] H. Hertz, D. E. Jones, and G. A. Schott, *Miscellaneous papers*. London: Macmillan, New York, Macmillan and co., 1896.
[2] K. L. Johnson, *Contact Mechanics*. Cambridge University Press, 1985.
[3] W. J. Stronge, *Impact Mechanics*, New Ed. Cambridge England; New York: Cambridge University Press, 2004.
[4] G. Gilardi and I. Sharf, "Literature survey of contact dynamics modelling," *Mech. Mach. Theory*, vol. 37, no. 10, pp. 1213–1239, 2002.
[5] K.-J. Bathe, *Finite Element Procedures*. Klaus-Jurgen Bathe, 2006.
[6] K.-J. Bathe, "Conserving energy and momentum in nonlinear dynamics: A simple implicit time integration scheme," *Comput. Struct.*, vol. 85, no. 7–8, pp. 437–445, Apr. 2007.
[7] V. Chawla and T. A. Laursen, "Energy consistent algorithms for frictional contact problems," *Int. J. Numer. Methods Eng.*, vol. 42, no. 5, pp. 799–827, Jul. 1998.
[8] B. Tchamwa, "Contribution à l'étude des méthodes d'intégration directe explicites en dynamique non linéaire des structures," Thèse, Nantes, 1997.
[9] H. B. Khenous, "Problèmes de contact unilatéral avec frottement de Coulomb en élastostatique et élastodynamique. Etude mathématique et résolution numérique.," Thesis, Institut National des Sciences Appliquées de Toulouse, 2005.
[10] T. Thenint, "Etude d'un système non linéaire à chocs sous excitation large bande : application à un tube de générateur de vapeur," phdthesis, Ecole Centrale Paris, 2011.
[11] M. Jean, "The non-smooth contact dynamics method," *Comput. Methods Appl. Mech. Eng.*, vol. 177, no. 3, pp. 235–257, Jul. 1999.
[12] T. Schindler and V. Acary, "Timestepping schemes for nonsmooth dynamics based on discontinuous Galerkin methods: Definition and outlook," *Math. Comput. Simul.*, vol. 95, pp. 180–199, Jan. 2014.
[13] C. Thornton, "Coefficient of Restitution for Collinear Collisions of Elastic-Perfectly Plastic Spheres," *J. Appl. Mech.*, vol. 64, no. 2, pp. 383–386, Jun. 1997.
[14] W. Goldsmith, *Impact: the theory and physical behaviour of colliding solids*. London: E. Arnold, 1960.
[15] C. M. Donahue, C. M. Hrenya, A. P. Zelinskaya, and K. J. Nakagawa, "Newton's cradle undone: Experiments and collision models for the normal collision of three solid spheres," *Phys. Fluids 1994-Present*, vol. 20, no. 11, p. 113301, Nov. 2008.
[16] J. Antunes, "Methods for the Dynamical Analysis of Nonlinear Structures," IPSI, Paris, France, 1991.
[17] Commissariat à l'énergie atomique (CEA), "Cast3m, Finite Element Software." [Online]. Available: www.cast3M.cea.fr.
[18] C. Behn, C. Will, and J. Steigenberger, "Unlike Behavior of Natural Frequencies in Bending Beam Vibrations with Boundary Damping in Context of Bio-inspired Sensors," presented at the INTELLI 2014, 2014, pp. 75–84.
[19] B. Nath Datta, "Numerical methods for the root finding problem." Northern Illinois University, 2013.
[20] N. F. Rieger, "The relationhip between finite element analysis and modal analysis.," *Sound Vib. 20*, p. 16, 1986.
[21] E. Boyere, "Modélisation des chocs et du frottement en analyse transitoire par recombinaison modale." Notice Code ASTER, 27-Jan-2010.
[22] B. Magnain, "Développement d'algorithmes et d'un code de calcul pour l'étude des problèmes de l'impact et du choc," phdthesis, Université d'Evry-Val d'Essonne, 2006.